The 8th European Congress on Computational Methods in Applied Sciences and Engineering
ECCOMAS Congress 2022
5 – 9 June 2022, Oslo, Norway

PROS AND CONS OF VARIOUS EQUIVALENT FRAME MODELS FOR NONLINEAR ANALYSIS OF URM BUILDINGS

AMIRHOSEIN SHABANI[*] AND MAHDI KIOUMARSI[†]

[*] Department of Civil Engineering and Energy Technology
Oslo Metropolitan University
Pilestredet 35, 0166, Oslo, Norway
e-mail: amirhose@oslomet.no, https://www.oslomet.no/om/ansatt/amirhose/

[†] Department of Civil Engineering and Energy Technology
Oslo Metropolitan University
Pilestredet 35, 0166, Oslo, Norway
e-mail: mahdik@oslomet.no, https://www.oslomet.no/om/ansatt/mahdik/

Key words: Equivalent Frame model, Macroelement, Nonlinear Analysis, Unreinforced Masonry, DM-MVLEM, Seismic Fragility.

Abstract. Brick masonry is considered as one of the old construction materials, and several cultural heritage assets are made of unreinforced masonry (URM), which is susceptible to earthquakes due to its brittle behavior. The equivalent frame method (EFM) is a nonlinear modeling method widely utilized for the seismic analysis of URM buildings with lower computational efforts than finite and discrete element methods. In this study, three macroelements, including the unified method (UM), composite spring method (CSM), and double modified multiple vertical line element model (DM-MVLEM), were utilized to model three case studies. The first case study is a full-scale two-story URM wall that was tested by applying the cyclic prescribed displacements, and two other case studies were developed by changing the configuration of openings. The second case study is with short piers, and weak spandrels exist in the third model. The efficiency of the methods in terms of the accuracy of the pushover results, prediction of damage patterns, and duration of the incremental dynamic analysis (IDA) are discussed. Finally, seismic fragility curves are provided to compare the IDA results.

1 INTRODUCTION

Recently, developing an integrated resilience assessment platform by utilizing a fast, adapted, and efficient multi-hazard risk assessment tool has gained acceptance for the sustainable reconstruction of historic areas [1]. Although different simplified analytical methods have been proposed to assess the vulnerability of unreinforced masonry (URM) buildings at a large scale, by developing computer technology and emerging supercomputers, accurate and fast nonlinear modeling approaches should be utilized for the near-real-time assessment or prediction of seismic risk purposes with a lower level of uncertainty [2]. Moreover, simplified methods could be necessary tools for the seismic analysis of buildings for designers who lack specialized skills. The equivalent frame method (EFM) is considered as the

most efficient method for nonlinear analysis of URM buildings [3]. Figure 1 shows the number of published journal articles regarding the EFM based on the related keywords searched in the Scopus database. The evolution of different macroelement models and their applications for seismic analysis of buildings with unreinforced masonry walls depicts the significance and the efficiency of the EFM.

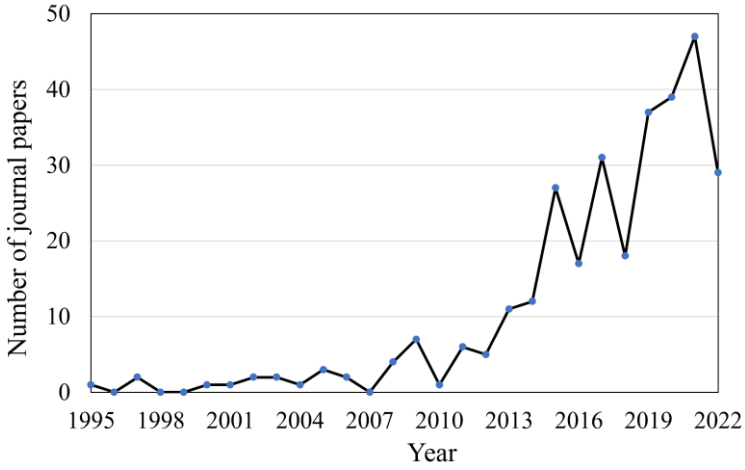

Figure 1: Number of relevant published journal papers since 1995 adapted from Scopus.

Various macroelements were developed to represent the nonlinear behavior of URM pier and spandrels, in which the unified method (UM) is considered one of the most simplified macroelements [4]. The main concept of UM is to model each URM wall in each story with a macroelement. The macroelement was then modified using the equivalent height method (EHM) for calculating the initial in-plane stiffness of the perforated URM walls [5, 6]. Shear and rocking hinges were employed at the middle and two sides of the elastic beam-column elements, respectively representing the failure modes and nonlinear behavior of masonry piers and spandrels in [7, 8]. As a simplified version, the composite spring method (CSM) was developed [3, 5]. Each pier can be modeled using a nonlinear shear spring with a specific backbone curve and ignoring the nonlinear behavior of spandrel elements. Fiber elements were also utilized to represent the nonlinear behavior of URM structural components considering the effect of axial-flexural interaction (N-M) [9, 10]. DM-MVLEM was developed considering the N-M effects with a lower computational effort than the fiber elements [3]. DM-MVLEM consists of two modified MVLEM elements available in OpenSees [11]. Two modified MVLEM elements are tied with a zero-length element to simulate the nonlinear shear behavior of the URM segments [3].

Seismic risk analysis should be performed to define the most vulnerable structures and determine the most efficient strategy for retrofitting the existing structures. The seismic fragility curves can be utilized to evaluate the expected social and economic losses [12]. Fragility is structure-specific and depends on the structure's design properties and condition. More specifically, fragility is defined as the probability of a structure reaching or exceeding a definite limit state subjected to an earthquake with an intensity level [13]. The fragility curves can be derived based on empirical, analytical, or hybrid methods. Around 64% of the literature studies from 2005-2021 related to seismic fragility analysis utilized analytical methods, and only 10% of the studies are related to the URM buildings [14]. Derivation of fragility curves based on the

IDA is one of the most accurate analytical methods [15]. Although this method is computationally demanding compared to other analytical methods, no prior assumptions are required regarding the probabilistic distribution of seismic demand for the derivation of fragility functions [16].

In this study, the UM, CSM, and DM-MVLEM were utilized to develop the nonlinear models of three case studies with different configurations of openings. The UM and DM-MVLEM are considered as the simplest and the most detailed methods, respectively. To investigate the accuracy of the methods, pushover analysis and IDA were carried out. The efficiency of the methods in terms of the accuracy of the pushover curves, prediction of damage patterns, and duration of the incremental dynamic analysis (IDA) are discussed. Furthermore, fragility curves were provided based on the IDA results by determining the record-to-record variability and modeling uncertainties, and the curves were compared to each other.

2 DEVELOPMENT OF NONLINEAR MODELS

Three case studies with different configurations of openings were modeled based on the UM, CSM, and DM-MVLEM. Therefore, nine nonlinear models were developed, and more details about the modeling based on each method in the OpenSees framework are presented in the following sections.

2.1 Unified method (UM)

The unified method (UM) was developed for the nonlinear analysis of confined and unconfined masonry walls. The UM macroelement consists of two truss elements at the two ends of the wall with linear behavior and a nonlinear shear spring in the middle of a wall. A nonlinear material with a trilinear backbone curve can be assigned to the lateral degree of freedom of the UM macroelement, and the other two degrees are free [4]. For this aim, two node link element and the hysteretic material model, available in the OpenSees library, were utilized. The maximum lateral strength of an unconfined URM wall can be calculated based on an equation that is not validated to calculate the value in the presence of the openings [4]. Another strategy was proposed to derive the maximum lateral strength by considering a weak connection between the piers and spandrels [3]. This conservative approach corresponds to the cantilever idealization in which null shear strength is considered for the spandrels. The maximum lateral strength is the sum of the maximum lateral strength of the vertical URM segments. The initial in-plane stiffness of URM walls with openings can be calculated based on the EHM. The EHM is a simplified analytical method that considers the flexibility of the two ends of piers due to the presence of spandrels for calculating the initial in-plane stiffness of URM walls with openings [6]. Details about the backbone curve and hysteresis parameters are presented in [3].

2.2 Composite spring method (CSM)

CSM is more accurate than the UM by discretizing perforated URM walls into piers and spandrels that are connected with the rigid elements based on the Dolce method [17]. The two node link element with a linear axial stiffness, fixed rotational degree of freedom, and a nonlinear shear spring were utilized to model a pier. The maximum lateral strength of piers is defined as the minimum value of the lateral strength due to shear sliding (V_s), diagonal cracking

(V_D), and rocking (V_R) failure modes [3]. The failure modes of piers can be roughly estimated by calculating the maximum lateral strength of each pier and defining the corresponding failure mode, which cannot be predicted using the UM. The initial in-plane stiffness of piers can be calculated based on the deep beam theory assumption by combining the shear and flexural stiffness of a wall with fixed-fixed boundary conditions [6]. Other specifications of the nonlinear shear spring are similar to unperforated walls presented for the UM macroelement elaborated in [3]. Note that, in this model, the nonlinear behavior of spandrel elements is not taken into account by modeling them using elastic beam-column elements.

2.3 Double modified MVLEM (DM-MVLEM)

Considering the nonlinearity in the spandrel element, N-M interaction effects, and prediction of the combined shear and flexural failure modes, DM-MVLEM is the most accurate macroelement used in this study. The DM-MVELM consists of two modified MVLEM connected with a zero-length element as a nonlinear shear spring [3]. The number of fiber elements is equal on two sides of the connection nodes of the MVLEM [18]. Therefore, the MVLEM elements cannot be used to simulate the asymmetrical segments that are common for URM spandrels. Furthermore, MVLEM elements cannot be utilized for modeling in the horizontal direction, and for modeling spandrel elements, the MVLEM elements should be modeled manually. For this aim, truss elements simulate the fiber elements of the MVLEM elements and connect two rigid parts to simulate the original MVLEM element for simulating the spandrels. Concrete 02 or Concrete 03 material with the stress-strain curve of masonry and the hysteretic material with a trilinear backbone curve can be assigned to the elements. Note that the former is assigned to the MVLEM fibers of piers and truss elements of spandrels, and the latter is assigned to the transitional degree of freedom of zero-length elements in the transverse direction to simulate the nonlinear shear behavior of the segments. The maximum lateral strength of the pier elements can be determined as the minimum value of the V_s and V_D based on [3]. Note that the maximum lateral strength of spandrels is determined as the minimum value of the V_D and the interlocking strength at bed joints at the intersection between spandrel and piers (V_I) based on [19]. The shear stiffness of the wall considering the deep beam theory for a pier with fixed-fixed boundary conditions can be considered as the initial in-plane stiffness of the zero-length elements [6].

2.4 Nonlinear models of full-scale URM walls

A full-scale two-story URM wall with openings tested at the University of Pavia (case study A) was considered the benchmark model in this study, see [20]. Case studies B and C were developed by changing the opening size of the benchmark model. Case study B is with an asymmetric configuration of openings and short piers, and case study C is with weak spandrels as illustrated in Figure 2 (a). All the case studies were modeled based on the DM-MVLEM, CSM, and UM as shown in Figure 2 (b), (c), and (d), respectively. Note that the UM models are the same based on the same length and height of the floor walls. Stress-strain curve of the URM material is depicted in Figure 2 (e) with the diagonal tensile strength (f_{td}) of 0.21 MPa and the shear strength of the masonry at zero compressive stress (f_{v0}) of 0.345 MPa based on [20].

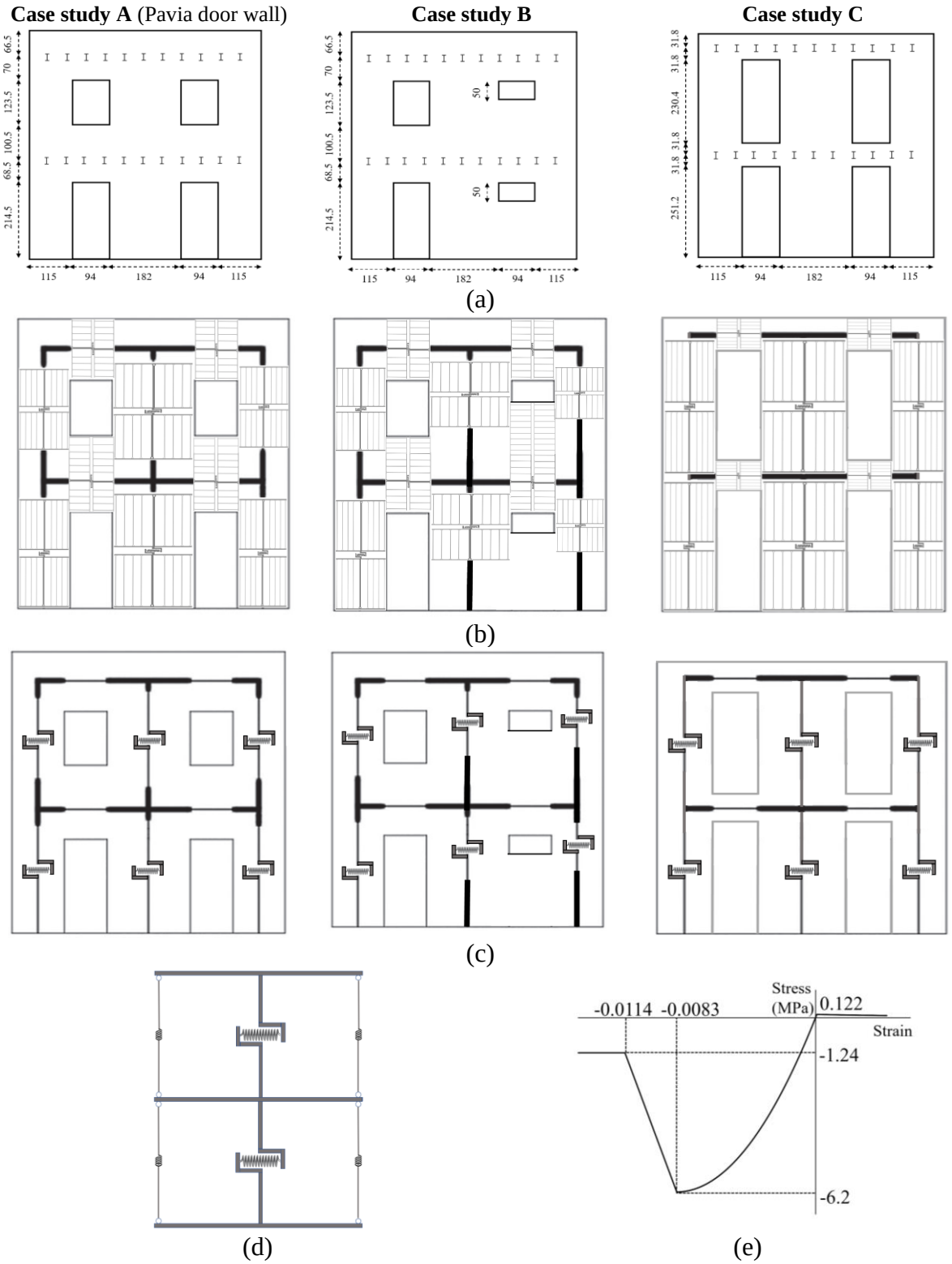

Figure 2: (a) Geometry of the case studies and the configuration of openings, (b) DM-MVLEM, (c) CSM, (d) UM models of the case studies, and (e) stress-strain curve of masonry.

3 PUSHOVER ANALYSIS

The pushover analysis was performed by applying the load pattern of the test for the Pavia door wall to compare the results with the test results and mass distribution load pattern for the other two case studies. The POA results are illustrated in Figure 17 for three case studies modeled according to the three aforementioned modeling approaches.

The Pavia door wall is the first case study, and the POA results show good agreement of the CSM and DM-MVLEM with the test results for deriving the pushover curve, as highlighted in Figure 3 (a) [20]. However, due to the conservative approach of the UM for calculating maximum shear strength by assuming weak connections of spandrels to piers, the pushover curve is conservative compared to the test result. For the case study B, with short piers and asymmetric opening configurations, pushover curves are close in the elastic phase. However, the post-peak behavior of the DM-MVLEM is more conservative than the CSM, see Figure 3 (b). Since the nonlinear behavior of spandrels was considered in the DM-MVELM, for the case study C, the pushover curves of the UM and DM-MVLEM models are close to each other, see Figure 3 (c). Nevertheless, the ultimate lateral strength is overestimated for the CSM model.

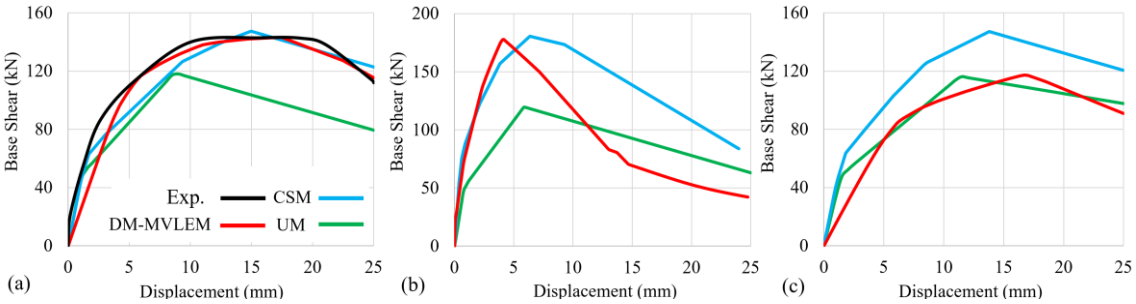

Figure 3: Pushover curves of (a) case study A (with the backbone curve from the test results [20]), (b) case study B, and (c) case study C.

3.1 Damage pattern prediction

In order to compare the failure modes occurring in the case studies, the damage patterns for the DM-MVLEM and CSM models by performing a monotonic POA are illustrated in Figure 4. Figure 4 (a) illustrates the damage pattern of the tested wall subjected to the cyclic displacements. The damage patterns for the Pavia door wall show that the CSM model cannot reflect the combined shear-flexural failure mode, as seen in the test, but this is reflected in the DM-MVLEM model, as illustrated in Figure 4 (b). Thus, the diagonal shear failure mode that can be seen in the test is not observed in the CSM model. Results from the failure modes representation of case study B show that the CSM can reflect the shear failure modes (which usually occurs in short piers) in good agreement with the DM-MVLEM as shown in Figure 4 (b). The failure of the spandrels was critical for case study C due to the presence of weak spandrels. Damage to spandrels has been predicted in the DM-MVLEM model but does not occur in the CSM due to the assumption of considering linear spandrel elements. Furthermore, combined shear-flexural failure modes cannot be defined using the CSM.

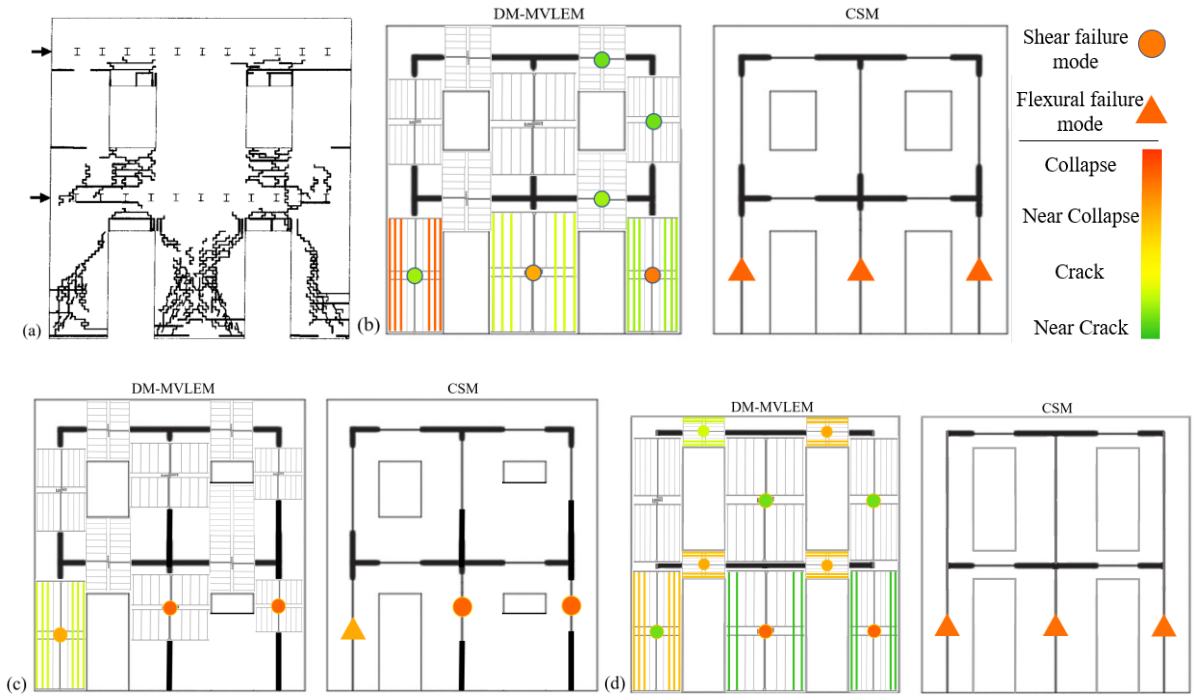

Figure 4: Damage patterns of the (a) tested wall [20], CSM, and DM-MVLEM models of the (b) case study A, (c) case study B, and (d) case study C.

4 INCREMENTAL DYNAMIC ANALYSIS (IDA)

For performing the IDA, an equivalent damping ratio of 2% at the first and second modal frequencies was considered proportional to the mass and the last committed stiffness matrix [3, 21]. Twenty-two pairs of far-field seismic records from the FEMA-P 695 guideline [22] were chosen, and the IDA was done by increasing the intensity of the records until the target limit state. The inter-story drift of 1% was considered for the collapse limit state [23].

The analysis duration and the average values for the models developed based on the methods are illustrated in Figure 5. The UM is the fastest method with the lowest computational effort. The analysis time of the UM and CSM models is 21% and 7% faster than DM-MVLEM models.

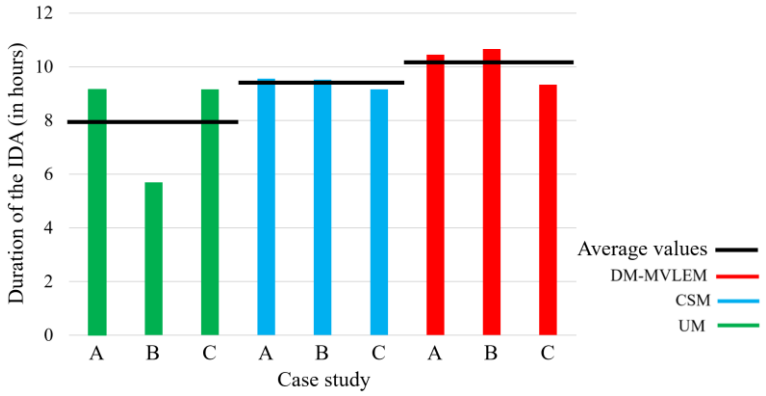

Figure 5: Duration of the IDA analysis of case study developed based on the UM, CSM, and DM-MVLEM.

An IDA curve is a diagram of the ground motion intensity measure (IM) against an engineering demand parameter (EDP). The IM and EDP are the spectral acceleration corresponding to the first mode elastic vibration period of the structure considering 5% of damping (Sa (T_1, 5%)) and the maximum inter-story drift, respectively [21]. Figure 6 shows the result of the IDA of the case studies modeled using the three methods.

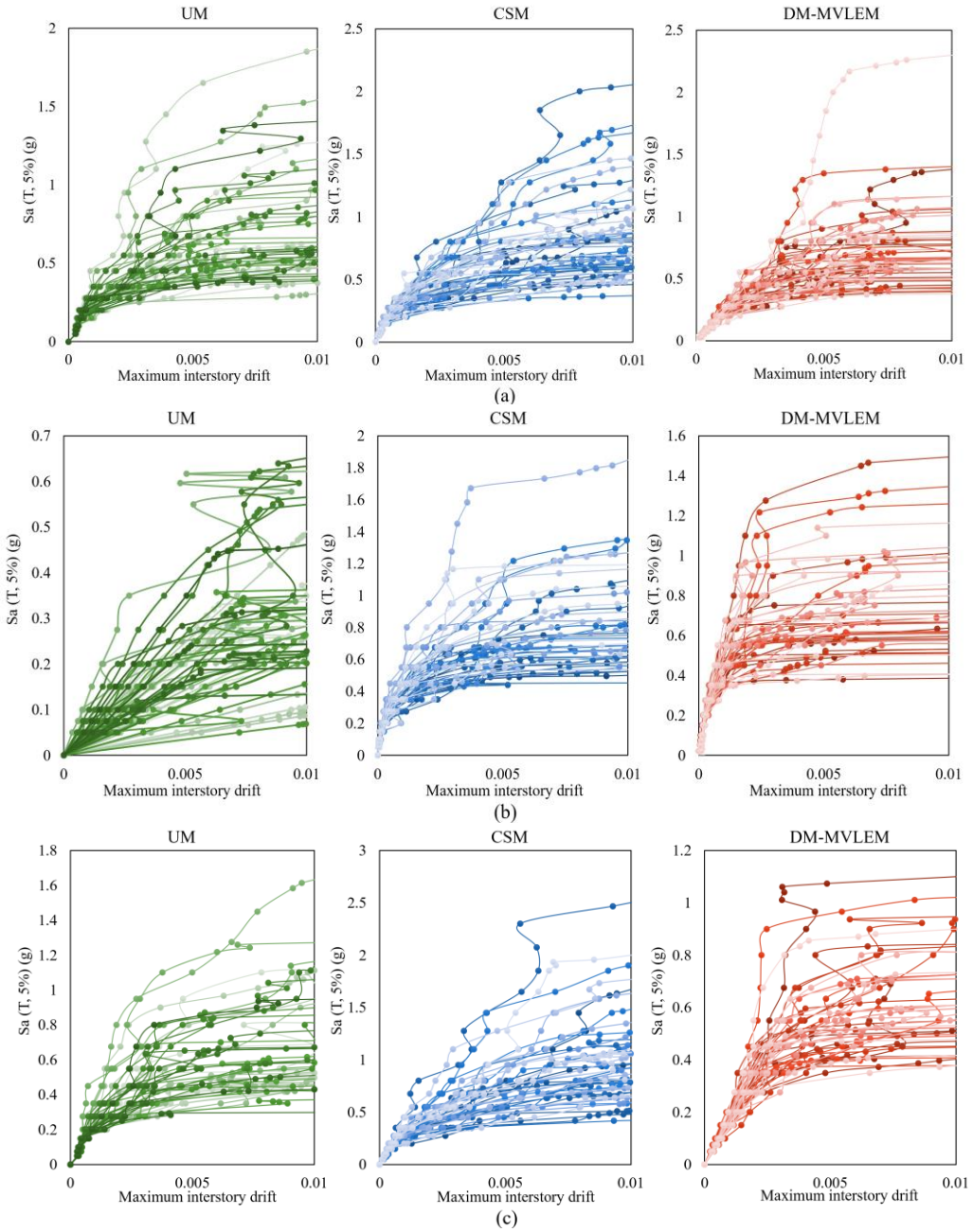

Figure 6: IDA curves of (a) Pavia door wall, (b) case study 2, and (c) case study 3 modeled based on the UM, CSM and DM-MVLEM.

5 SEISMIC FRAGILITY ANALYSIS

This study uses a lognormal cumulative distribution function to define a fragility function based on Equation (1).

$$P[C|IM = im] = \Phi\left[\frac{ln(im) - \eta}{\beta}\right] \quad (1)$$

where $P[C|IM = im]$ is the probability that a ground motion with $IM = im$ will cause the structure to collapse. $\Phi()$ is the standard normal cumulative distribution function, $ln()$ is the natural logarithm function, η and β are the mean and standard deviation, respectively, of the $ln(im)$ values . In order to incorporate the modeling uncertainty in the seismic fragility analysis, the β value is calculated based on Equation (2), considering both the record-to-record variability and the modeling uncertainty [24].

$$\beta = \sqrt{\beta_M^2 + \beta_D^2} \quad (2)$$

where β_D is the dispersion associated with uncertainty in demand (record-to-record variability) which is calculated as the mean of the $ln(im)$ values and β_M is the modeling uncertainty. The predefined β_M values represent collapse characteristics, and the accuracy and robustness of the models can be derived from [22].

Considering a medium level for the representation collapse characteristics of the case studies, the β_M values are assigned to each modeling approach based on Table 1. The low level of the accuracy was assigned to the UM, due to the cantilever idealization and the simplified formulation of the modeling approach. But piers and spandrels were modeled separately based on CSM, and different equations were proposed to define the maximum lateral strength. Nevertheless, the inelastic behavior of the spandrel elements is ignored, the N-M interaction is not taken into account, explicit hysteresis behaviors for different in-plane failure modes are not considered and the combined shear-flexural failure modes cannot be predicted using the CSM. Hence the medium level of accuracy of the model can be assigned to the CSM. All the aforementioned shortcomings of the CSM were modified in the DM-MVLEM, but the N-V interaction is not considered during the nonlinear analysis, and the high accuracy level is assigned to the DM-MVLEM.

Table 1: The quality rating of archetype models

The level of accuracy and robustness	High	Medium	Low
Description	Nonlinear models simulate all predominant inelastic effects with robust computational solution algorithms.	Nonlinear models capture most nonlinear deterioration and response mechanisms leading to collapse.	Nonlinear models capture the onset of yielding and subsequent strain hardening but do not simulate the degrading response and capture the effects of deterioration and redistribution.
β_M	0.2	0.35	0.5

All the uncertainty values for the models are presented in Table 2 and fragility curves are illustrated in Figure 7. The fragility curves derived from the analysis of UM and CSM with the higher uncertainty values, as presented in Table 2, are flatter than the curves of the DM-MVLEM models. The fragility curves of case study A are close to each other without a considerable change. For case study B, the results of the fragility analysis of the UM are more conservative than the other two approaches. The curves of case study B for the CSM and DM-MVLEM are close to each other. Moreover, for case study C, the median values of the IM for the UM and DM-MVLEM models are close to each other; however, the differences are due to the higher level of uncertainty of UM and the IM that causes damage is overestimated for the CSM model. Considering the collapse margin ratio of 10% based on [22], UM and CSM are considered the most and the least conservative approaches, respectively. The IM values for the CSM and DM-MVLEM models are close to each other for the 10% of collapse margin ratio.

Table 2: Calculated parameters of the fragility curves, including the uncertainty values

Modeling type	Name of the case study	η	β_D	β_M	β
UM	Case study A	-0.432	0.412	0.5	0.648
	Case study B	-1.336	0.51	0.5	0.715
	Case study C	-0.423	0.379	0.5	0.627
CSM	Case study A	-0.229	0.387	0.35	0.522
	Case study B	-0.255	0.318	0.35	0.473
	Case study C	-0.067	0.406	0.35	0.536
DM-MVLEM	Case study A	-0.354	0.383	0.2	0.432
	Case study B	-0.355	0.32	0.2	0.377
	Case study C	-0.515	0.284	0.2	0.347

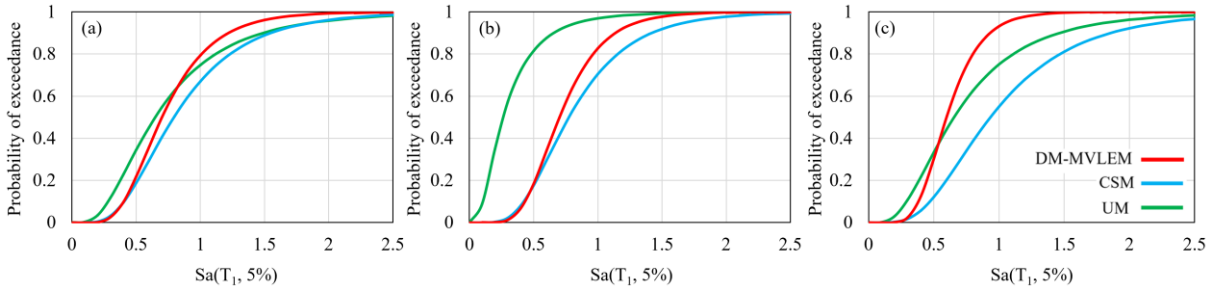

Figure 7: Seismic fragility curves of the (a) case study A, (b) case study B, and (c) case study C.

6 CONCLUSIONS

- Except for case study C with weak spandrels, the pushover curve of UM models is conservative in terms of the ultimate base shear. However, due to neglecting the nonlinear behavior in the CSM, the results overestimate the maximum base shear for case study C, and the UM results are in good agreement with the DM-MVLEM.
- Damage patterns cannot be predicted using the UM. Moreover, DM-MVLEM is more accurate than the CSM by highlighting the combined flexural-shear failure modes and prediction of the failure of spandrels. However, the shear failure modes can be

predicted based on the CSM, which usually can be observed in short piers.

- UM is considered the fastest method for performing IDA with the highest level of uncertainty, and DM-MVLEM is the opposite. Results of the IDA were summarized in the fragility curves by incorporating the effect of record-to-record variability and modeling uncertainty. The fragility curves derived from the UM and CSM are flatter than DM-MVLEM due to the higher level of uncertainty. CSM cannot be a robust method in case of existing weak spandrels.

ACKNOWLEDGMENT

This work is a part of the HYPERION project. HYPERION has received funding from the European Union's Framework Programme for Research and Innovation (Horizon 2020) under grant agreement No 821054. The contents of this publication are the sole responsibility of Oslo Metropolitan University (Work Package 5, Task 2) and do not necessarily reflect the opinion of the European Union.

REFERENCES

[1] Shabani, A., Skamantzari, M., Tapinaki, S., Georgopoulos, A., Plevris, V., and Kioumarsi, M. 3D simulation models for developing digital twins of heritage structures: challenges and strategies. *Procedia Struct. Integr.*, (2022), **37**: p. 314-320, https://doi.org/10.1016/j.prostr.2022.01.090.

[2] Shabani, A., Kioumarsi, M., and Zucconi, M. State of the art of simplified analytical methods for seismic vulnerability assessment of unreinforced masonry buildings. *Eng. Struct.*, (2021), **239**: p. 112280, https://doi.org/10.1016/j.engstruct.2021.112280.

[3] Shabani, A. and Kioumarsi, M. A novel macroelement for seismic analysis of unreinforced masonry buildings based on MVLEM in OpenSees. *J. Build. Eng.*, (2022), **49**: p. 104019, https://doi.org/10.1016/j.jobe.2022.104019.

[4] Xu, H., Gentilini, C., Yu, Z., Wu, H., and Zhao, S. A unified model for the seismic analysis of brick masonry structures. *Constr Build Mater.*, (2018), **184**: p. 733-751, https://doi.org/10.1016/j.conbuildmat.2018.06.208.

[5] Park, J. Investigation of the Geometric Variation Effect on Seismic Performance of Low-Rise Unreinforced Masonry Structures Through Fragility Analysis. *Int. J. Civ. Eng.*, (2018), **16**(1): p. 93-106, https://doi.org/10.1007/s40999-016-0070-x.

[6] Shabani, A., Plevris, V., and Kioumarsi, M. *A Comparative Study on the Initial In-plane Stiffness of Masonry Walls with Openings*. Proceedings of the World Conference on Earthquake Engineering, 17WCEE, Sendai, Japan. (2021).

[7] Pasticier, L., Amadio, C., and Fragiacomo, M. Non-linear seismic analysis and vulnerability evaluation of a masonry building by means of the SAP2000 V. 10 code. *Earthq Eng Struct Dyn*, (2008), **37**(3): p. 467-485.

[8] Petrovčič, S. and Kilar, V. Seismic failure mode interaction for the equivalent frame modeling of unreinforced masonry structures. *Eng. Struct.*, (2013), **54**: p. 9-22, https://doi.org/10.1016/j.engstruct.2013.03.050.

[9] Siano, R., Roca, P., Camata, G., Pelà, L., Sepe, V., Spacone, E., and Petracca, M. Numerical investigation of non-linear equivalent-frame models for regular masonry walls. *Eng. Struct.*, (2018), **173**: p. 512-529, https://doi.org/10.1016/j.engstruct.2018.07.006.

[10] Peruch, M., Spacone, E., and Camata, G. Nonlinear analysis of masonry structures using fiber-section line elements. *Earthq Eng Struct Dyn*, (2019), **48**(12): p. 1345-1364, https://doi.org/10.1002/eqe.3188.
[11] Mazzoni, S., McKenna, F., Scott, M.H., and Fenves, G.L. *OpenSees command language manual*. Pacific Earthquake Engineering Research (PEER) Center, USA. (2006).
[12] Shabani, A., Alinejad, A., Teymouri, M., Costa, A.N., Shabani, M., and Kioumarsi, M. Seismic Vulnerability Assessment and Strengthening of Heritage Timber Buildings: A Review. *Buildings*, (2021), **11**(12): p. 661.
[13] Silva, V., Akkar, S., Baker, J., Bazzurro, P., Castro, J.M., Crowley, H., Dolsek, M., Galasso, C., Lagomarsino, S., Monteiro, R., Perrone, D., Pitilakis, K., and Vamvatsikos, D. Current Challenges and Future Trends in Analytical Fragility and Vulnerability Modeling. *Earthq. Spectra*, (2019), **35**(4): p. 1927-1952, https://doi.org/10.1193%2F042418EQS101O.
[14] Rajkumari, S., Thakkar, K., and Goyal, H. Fragility analysis of structures subjected to seismic excitation: A state-of-the-art review. *Structures*, (2022), **40**: p. 303-316, https://doi.org/10.1016/j.istruc.2022.04.023.
[15] Muntasir Billah, A.H.M. and Shahria Alam, M. Seismic fragility assessment of highway bridges: a state-of-the-art review. *Struct. Infrastruct. Eng.*, (2015), **11**(6): p. 804-832, https://doi.org/10.1080/15732479.2014.912243.
[16] Zhang, J. and Huo, Y. Evaluating effectiveness and optimum design of isolation devices for highway bridges using the fragility function method. *Eng. Struct.*, (2009), **31**(8): p. 1648-1660.
[17] Cattari, S., D'Altri, A.M., Camilletti, D., and Lagomarsino, S. Equivalent frame idealization of walls with irregular openings in masonry buildings. *Eng. Struct.*, (2022), **256**: p. 114055, https://doi.org/10.1016/j.engstruct.2022.114055.
[18] Orakcal, K., Wallace, J.W., and Conte, J.P. Flexural modeling of reinforced concrete walls-model attributes. *Structural Journal*, (2004), **101**(5): p. 688-698.
[19] Rinaldin, G., Amadio, C., and Gattesco, N. Review of experimental cyclic tests on unreinforced and strengthened masonry spandrels and numerical modelling of their cyclic behaviour. *Eng. Struct.*, (2017), **132**: p. 609-623, https://doi.org/10.1016/j.engstruct.2016.11.063.
[20] Magenes, G., Kingsley, G.R., and Calvi, G.M. *Seismic testing of a full-scale, two-story masonry building: test procedure and measured experimental response*. Consiglio nazionale delle ricerche, Gruppo nazionale per la Difesa dai terremoti. (1995).
[21] Vamvatsikos, D. and Cornell, C.A. Incremental dynamic analysis. *Earthq Eng Struct Dyn*, (2002), **31**(3): p. 491-514, https://doi.org/10.1002/eqe.141.
[22] FEMA. *Quantification of Building Seismic Performance Factors, FEMA P695*. Federal Emergency Management Agency: United States, Washington, D.C. (2009).
[23] FEMA. *Prestandard and Commentry for the Seismic Rehabilitaion of Buildings, FEMA 356*. Federal Emergency Management Agency: Washington, D.C. (2000).
[24] D'Ayala, D., Meslem, A., Vamvatsikos, D., Porter, K., and Rossetto, T. *Guidelines for analytical vulnerability assessment: Low/mid-rise, GEM vulnerability and loss modelling*. Global Earthquake Model (GEM) Foundation, Pavia. (2015).